# Magic angles and cross-hatching instability in hydrogel fracture

T. Baumberger, C. Caroli, D. Martina, and O. Ronsin
*INSP, UPMC Univ Paris 06, CNRS UMR 7588 140 rue de Lourmel, 75015 Paris France*
(Dated: February 29, 2008)

The full 2D analysis of roughness profiles of fracture surfaces resulting from quasi-static crack propagation in gelatin gels reveals an original behavior characterized by (i) strong anisotropy with maximum roughness at $V$-independent symmetry-preserving angles, (ii) a sub-critical instability leading, below a critical velocity, to a cross-hatched regime due to straight macrosteps drifting at the same magic angles and nucleated on crack-pinning network inhomogeneities. Step height values are determined by the width of the strain-hardened zone, governed by the elastic crack blunting characteristic of soft solids with breaking stresses much larger that low strain moduli.

PACS numbers: 62.20.Mk, 83.80.Kn



Over the past two decades, considerable effort has been devoted to characterizing and understanding the statistical properties of the roughness of fracture surfaces in linear elastic disordered materials. Investigation of a wide variety of systems, ranging from brittle silica glass to ductile metallic alloys, has revealed the ubiquity of wide roughness spectra exhibiting self-affine characteristics on sizeable wavelength ranges. On the basis of analysis of height-height correlation functions in a single direction, E. Bouchaud *et al.* [1] first conjectured a fully universal behavior summed up into a single Hurst exponent. The discrepancies between the predictions of various subsequent theoretical models have pointed toward the importance of also investigating possible anisotropies of the scaling properties [2]. Work along this line indeed reveals different scaling exponents along the crack propagation direction and the (orthogonal) crack front one. From this, Ponson *et al.* [3] conclude that the self-affinity of the roughness is described by a Family-Vicsek scaling, hence by a set of two exponents. Within their new analysis, full universality is no longer the case since they evidence the existence of at least two classes of materials.

However, on the basis of their theoretical work, Bouchbinder *et al.* [4] have recently raised several new issues. In particular, they point to the necessity of a full 2D analysis of the correlations and find, when reexamining some experimental data, that a host of up to now unidentified exponents appear. They insist on the need to focus on the effects of departures from linear elasticity in the fracture process.

In this spirit we report here on the nature of surface morphologies resulting from the fracture of gelatin, a highly compliant thermally reversible hydrogel, in the strongly subsonic regime. We show that these surfaces present very striking anisotropic features. Namely, the rms roughness $R(\theta)$, measured along a direction at angle $\theta$ from the propagation one $Ox$, exhibits two symmetry-preserving maxima for $\theta = \pm\theta_m$. For gels with a fixed gelatin concentration, this "magic angle" $\theta_m$ is constant over more than one decade of both crack velocity $V$ and solvent viscosity $\eta$. Moreover, below a critical, $\eta$-dependent, velocity $V_c$ a new regime develops, characterized by a cross-hatched (CH) morphology analogous to those observed previously on a covalently cross-linked hydrogel [5, 6] and on various elastomers, swollen or not [7]. It is due to straight "macroscopic" steps, here of heights a few 100 $\mu$m, emerging from the above-described coexistent micrometric roughness. These steps are oriented at the same magic angles $\pm\theta_m$ as those revealed by the microroughness. Their growth results from a dynamical instability which we show to be subcritical: for $V > V_c$, while the inhomogeneities of the gel network are not strong enough to trigger step nucleation, we are able to force it with the help of externally applied local stress perturbations.

These results lead us to propose the existence of a new class of morphologies, characteristic of highly compliant random polymer networks with breaking stresses larger than their small strain Young modulus, in which fracture implies elastic crack blunting [9] and strong elastic nonlinearities at work in the near-tip region.

*Experimental* — Our fracture surfaces result from mode-I cracks propagating along the mid-plane of long, thin gelatin slabs (Fig. 1.a.), as described in detail in reference [10]. A displacement $\Delta$ of the rigid grips is imposed along $Oy$ to the notched plate. After an initial transient, the crack reaches a steady regime at a velocity $V$ which increases with the "energy release rate" $\mathcal{G}$ imposed by the opening $\Delta$. We found that, in this slow, subsonic regime ($V < 30$ mm/s):

$$\mathcal{G} = \mathcal{G}_0 + \Gamma\eta V \tag{1}$$

with $\mathcal{G}_0 \simeq 2.5$ J.m$^{-2}$, $\Gamma \simeq 10^6$, and were able to assign this strong $V$-dependence to the fact that, in such a reversible gel, fracture occurs via scissionless chain pull-out, the high dissipation being due to viscous drag [10, 11].

The results reported here were obtained on gels with a 5 wt.% content of gelatin in the solvent (pure water except when otherwise specified). The gel low-strain shear modulus $\mu = 3.5$ kPa (transverse sound speed $\sim 1.9$ m/s), is due to the entropic elasticity of the ran-

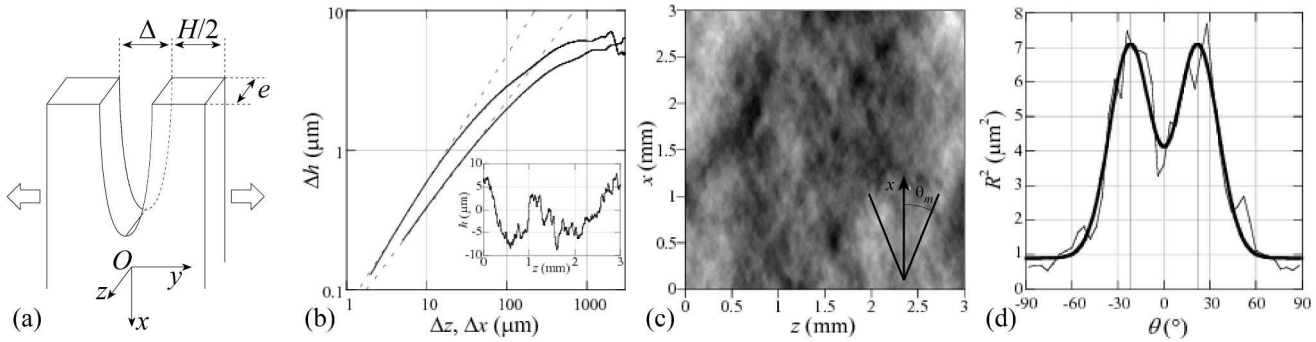


FIG. 1: Roughness characteristics for a 5 wt% gelatin/water gel for crack velocity $V = 13.5$ mm/s. (a) Experimental geometry. Sample dimensions : $H = 30$ mm, $e = 10$ mm, length $L = 300$ mm. (b) Height-height correlation functions $\Delta h_x(\Delta x)$ (lower curve) and $\Delta h_z(\Delta z)$ (upper curve). Inset : a typical profile along $Oz$. (c) $3 \times 3$ mm$^2$ map of heights $h(x, z)$. The gray scale ranges over $27\,\mu$m. The oblique lines correspond to peak positions in fig. 1.d. (d) Anisotropic squared roughness $R^2$ *vs.* angle $\theta$ measured from crack propagation direction. The dark line is the best fit with a sum of two gaussians with an offset baseline.

| tip velocity (mm.s$^{-1}$) | 1.16 | 5.9 | 13.5 | 23.3 |
|---|---|---|---|---|
| crack opening $\Delta$ (mm) | 5 | 7 | 9 | 11 |
| rms roughness ($\mu$m) | 2.5 | 3.1 | 4.1 | 5.3 |
| angle $\theta_m$ ($^\circ$) | 18 | 17 | 17 | 22 |

TABLE I:

dom polymer network, of average mesh size $\xi \sim 10$ nm. Note that, owing to this huge compliance, even very slow cracks ($V \sim 100\ \mu$m/s) demand large openings $\Delta$ (Table I), typically $\gtrsim 3$ mm. Post-mortem replicas of crack surfaces, obtained by UV curing of a thin layer of glue, are scanned with the help of a mechanical profilometer (stylus tip radius $2\,\mu$m, out of plane resolution 0.1 nm). Our maps $h(x, z)$ of heights above mean plane correspond to $3 \times 3$ mm$^2$ scans. Each one consists of a series of 600 lines parallel to the front direction $Oz$, each line containing 1500 data points.

*The microrough morphology* — For $V \gtrsim 300\ \mu$m/s, the fracture surfaces are flat on the macroscale, yet clearly not mirror-like. As expected with such a material, elastic modulus as well as toughness fluctuations due to the randomness of the network result in in- and out-of-plane excursions of the crack front line, the profile roughness being the imprint of the latter ones. A typical map is shown in figure 1.b. For this crack velocity $V = 13.5$ mm/s, we find that the global rms roughness $\bar{R} = 4.1\,\mu$m [12]. Following Ponson *et al.* [3], we first characterize height correlations along the front ($Oz$) i.e. we compute : $\Delta h_z(\Delta z) = \langle [h(z + \Delta z, x) - h(z, x)] \rangle_{z,x}^{1/2}$ and its counterpart $\Delta h_x(\Delta x)$ along the propagation direction ($Ox$). As indicated by figure 1.b. the microroughness spectrum is anisotropic and of the broad band type. However, at variance with the findings of [3], a simple power law fit (see dashed lines) is, here, clearly unconvincing. The discrepancy leads us, following Bouchbinder *et al.* [4], to try and exploit more extensively the full 2D information. Indeed, naked-eye inspection under grazing incidence, as well as the aspect of height maps (Fig. 1.c.), strongly suggest the presence of preferred oblique directions. This suspicion we have confirmed by computing the angle-dependent squared roughness $R^2(\theta)$, obtained by integrating the power spectrum $|\tilde{h}(\mathbf{q})|^2$ over an angular sector $d\theta = 4^\circ$ about angle $\theta + \pi/2$ (in $\mathbf{q}$-space) and in the wavelength window $2\,\mu$m–1 mm. We find in all cases that $R^2(\theta)$ exhibits two marked symmetric peaks at $\theta = \pm\theta_m$ (see figure 1.d. for which $\theta_m = 22^\circ$). Moreover (Table I), $\theta_m$ does not show any significant variation over the whole $V$-range ($V_{max}/V_{min} \sim 20$). In addition, a 10-fold increase of solvent viscosity $\eta$, obtained by using a 40/60 water/glycerol mixture, does not either affect its value.

Finally (see Table I), the full 2D-averaged rms roughness $\bar{R}$ clearly increases with the imposed crack opening $\Delta$, hence with $V$.

*The crosshatched (CH) morphology* — Starting from the microrough regime, we perform a step-by-step decrease of $\Delta$, thus slowing down crack propagation. Below a critical velocity $V_c = 350 \pm 20\,\mu$m/s we observe on the fracture surfaces the emergence, at apparently random locations across the slab width, of oblique straight line defects (Fig. 2.a.). Upon further $V$ decrease, these lines proliferate into a scale-like pattern, akin to the CH morphologies found by Tanaka *et al.* [5] on a covalently cross-linked gel and by Gent *et al.* [7] on elastomers.

Note that, since these observations pertain to the quasistatic regime, front wave propagation [8] is irrelevant here.

Profile analysis (Fig. 2.b.) shows that these lines correspond to steps which emerge via self-amplification of the microroughness, with which they coexist. Their height saturates, after a traveling distance of several millimeters, to values on the order of $200\,\mu$m. No change of

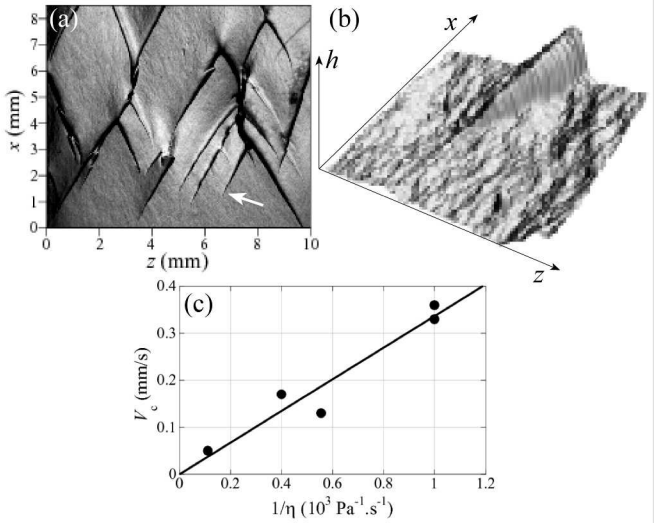


FIG. 2: Emergence of the CH regime. (a) A typical CH pattern close below $V_c$. The crack propagates upward. (b) 3D profile (400×400 $\mu$m$^2$, 15 $\mu$m peak to peak) the emergence of a macrostep (arrow on Fig. 2.a.) out of the microroughness. (c) Critical velocity $V_c$ vs. inverse viscosity for 5% gelatin gels in water/glycerol solvents. The line is the best linear fit.

their drift angle is discernable as they grow, so that they propagate at the magic angle $\theta_m$ of the microroughness. We find it to remain $V$-independent over the full $V < V_c$ explored range.

The large $\Delta$ values make it possible to image the crack surfaces in the tip region. Figures 3.a–d depict the emergence and growth of a defect, in a frame attached to the moving crack front. It is seen to drift along the front direction $Oz$ at a constant velocity $V_d$, as expected from the straightness of CH lines. So, as we have checked from *e.g.* Fig. 3.b-d., $V_d = V \tan\theta_m$. Fig. 3.e corresponds to the fully developed defect, schematized on Fig. 3.f. It shows that the crack front has become discontinuous, and composed of two semi-cracks $A_0A$, $B_0B$. As it moves along $Ox$, $A_0A$ creates two "lips" $\alpha_I$, $\alpha_{II}$. In the vicinity of its tip, the second semi-crack is delayed with respect to $A_0A$, so that its end point $B$ lies on the $\alpha_{II}$ lip. The defect topology thus involves a material overhang $ABC_ID_I$. Note that this topology is the equivalent, for a widely open crack, of that identified in [5] and [7]. As the front proceeds, the fold $A_IC_ID_IB_I$ ultimately collapses, leaving two complementary steps on the crack faces.

Finally, in order to shed light on the role of solvent viscosity $\eta$, we have studied gels made with water-glycerol mixtures. We find that the CH morphology persists but that the critical velocity $V_c$ scales as $1/\eta$ (Fig. 2.c). However, the magic angle $\theta_m$ is $\eta$-independent.

*Discussion* — The above phenomenology presents several striking discrepancies with the known morphologies, pertaining to metallic alloys, silica glasses, quasi-crystals, mortar, wood and sandstone [2]. Namely, none of these materials has been reported to exhibit (i) preferential anisotropy directions (ii) a CH regime (iii) a noticeable increase of $\bar{R}$ with $V$ in the quasistatic regime. On the other hand, these a priori puzzling features are not restricted to gelatin gels. Indeed, as already mentioned, the CH regime has been documented for a chemical hydrogel and for elastomers. Moreover, using figure 5 of reference [6], one easily checks that, in their chemical gel as well, the CH drift angle is constant ($\theta_m \simeq 43°$) over a 40-fold increase of $V$ up to a critical $V_c$ where the CH regime disappears.

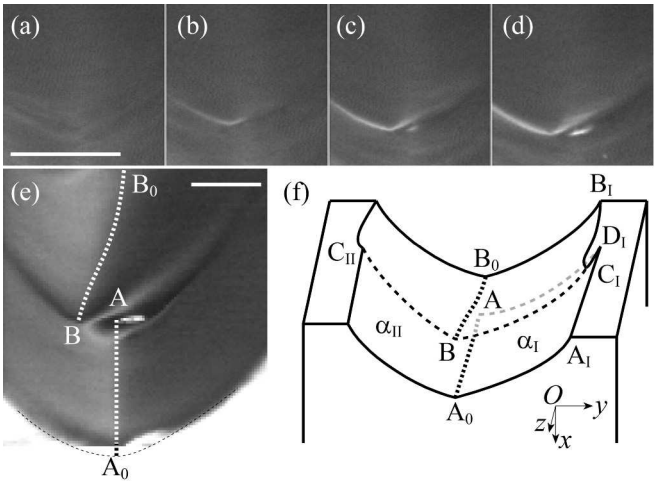


FIG. 3: Emergence and growth of a CH defect as viewed at 60° from $Ox$ in the $Oxz$ plane. White bar length : 200 $\mu$m (a)–(d) Snapshots at constant time intervals $\Delta t = 0.4s$ in the moving tip frame. The defect (bright line) grows and drifts at constant velocity. (e) Fully developed defect. The wite dashed lines mark the discontinuous front line. (f) Sketch of the defect topology.

The question then arises of which material features may be responsible for this new class of behavior. In view of the dependence of $V_c$ on solvent viscosity, one might be tempted to invoke poroelasticity. However Gent et al. have observed CH morphologies as well with dry elastomers as with a network swollen (ration 2.6) with oil. Hence the presence of solvent is not necessary for this regime to exist.

This apparent paradox has led us to investigate the nature of the transition at $V_c$. The fact that (i) the microroughness does not show any trend towards divergence when approaching $V_c$ from above, (ii) the height $\delta$ of CH steps does not vanish as $V \to V_c^-$, prompts that the CH instability is discontinuous, i.e. involves nucleation. If so, it should be possible to trigger CH steps above $V_c$ with the help of large enough external perturbations. Indeed, in a large range of $V > V_c$, inducing a mixed (II+III) mode stress perturbation by pinching the gel slab off midplane, slightly ahead of the tip, results in the nucleation

of a step that propagates through the sample.

So, $V_c$ appears as a threshold below which the structural noise due the randomness of the gel network is not strong enough for the step nucleation barrier to be overcome. This, together with the fact that $\eta V_c$ is a constant for a given network structure, suggests the following tentative picture: when the crack front meets a tougher zone (due to a local decrease $\delta\xi$ of meshsize $\xi$) of spatial extent $\gtrsim d_{act}$, with $d_{act} \approx 100$ nm the size of the process zone[10], it slows down locally, generating a wall which stretches as the crack lips open. We postulate that step nucleation demands that the tough zone pins the front down to a full stop, i.e. that the front velocity fluctuation $\delta V = -V_c$. According to the fracture model developed in refs. [10], [11], both $\mathcal{G}_0$ and $\Gamma$ in eq.(1) scale as $\xi^{-2}$. In the experiment, $\mathcal{G}$ is kept constant via the constancy of $\Delta$. So, $\eta\delta V = (\mathcal{G}/\Gamma)\delta\xi^2/\xi^2$. From this, we can estimate the maximum relative amplitude $\epsilon_m$ of mesh size fluctuations on spatial scales $\gtrsim d_{act}$ in our system as $\epsilon_m \approx \Gamma/2\mathcal{G}_0\eta V_c \approx 7\%$. The smallness of $\epsilon_m$ justifies our approximating $\mathcal{G}$ by $\mathcal{G}_0$ in this estimate and explains the quasi-constancy of $\eta V_c$. Such an order of magnitude is statically plausible, and at the same time compatible with the sizeable large-angle light scattering exhibited by our gels.

On the basis of this picture we interpret step nucleation as resulting from the pinning of a small part of the crack line. Due to local asymmetries, one of the resulting semi-cracks takes the lead, the other one getting delayed while skirting around the tough zone via an excursion towards the easier lip, thus nucleating the overhang. As cracking proceeds its endpoint $B$ is gradually advected away by the opening of the $A_0A$ crack (Fig. 3.f), until it gets far enough from $A_0A$ for tensile stresses along $\alpha_{II}$ to become negligible.

Now, our gelatin gels share with all the other soft solids exhibiting CH two mechanical characteristics: (i) the breaking stress is much larger than the low strain Young modulus $E$ (ii) they strain-harden considerably at large deformation levels where polymer segments are stretched quasi-taut[13]. Hui et al. [9] have shown that (i) entails elastic crack blunting while, due to (ii) stress concentration is restricted to a strain-hardened region of thickness $\sim \mathcal{G}/E$ along $Oy$. This allows us to predict that outward advection of $B$ stops when the distance from $B$ to $A_0A$, i.e. the step height $\delta$ becomes of order $\mathcal{G}_0/E$. With $\mathcal{G}_0 \approx 2.5$ J.m$^{-2}$, $E \approx 10$ kPa, we get $\delta \approx 150\,\mu$m, in excellent agreement with the experimental value. For slow cracks in elastomers as studied in [7], $\mathcal{G}_0$ and the relaxed $E$ are respectively of order a few 10 J.m$^{-2}$ and a few MPa, leading to step heights $\delta$ in the $10\,\mu$m range. This agrees with Gent's findings, lending further support to our picture.

Finally, let us reconsider the defect shape as depicted on Fig. 3.f. In its end region close to $A$ (i.e. for $z_A < z < z_B$), the lower semi-crack connects the stretched lip $\alpha_I$ with the ceiling of the fold, in which stresses are, to a large extent, relaxed by the $B_0B$ cut. This is consistent with the fact that, as cracking proceeds, $B_0B$ which cuts into the unscreened $\alpha_{II}$ lip, elongates ($B$ drifts) towards $z > 0$ while $A_0A$ regresses. This screening effect of the fold geometry explains that the defect drifts along the front in a direction defined by the initial symmetry-breaking choice which has led $B_0$ towards one or the other crack lip.

In the context of the above description, the existence of a preferred orientation in the micro-roughness could be attributed to aborted attempts at fold development. However, why $\theta_m$ is independent of both $V$ and the amplitude of out-of-plane excursions remains at this stage a fully open question.

In conclusion we propose that the phenomenology brought to light and analyzed here is characteristic, beyond the case of gelatin gels, of a new class of morphologies of fracture surfaces. The scenario which we propose to describe the cross-hatching instability implies that this class is characteristic of soft, tough, elastic materials which exhibit elastic crack-blunting and strong, strain-hardening, elastic non-linearities.

We are grateful to K. Sekimoto for stimulating interactions along the course of this work. We also thank M. Adda-Bedia, A. Argon, D. Bonamy, H. Brown, V. Lazarus for helpful discussions.

[1] E. Bouchaud, G. Lapasset, and J. Planès, Europhys. Lett. **13**,73 (1990).
[2] L. Ponson, *Crack propagation in disordered materials*, PhD Thesis, Ecole Polytechnique 2006 (unpublished).
[3] L. Ponson, D. Bonamy, and E. Bouchaud, Phys. Rev. Lett. **96**, 035506 (2006).
[4] E. Bouchbinder, I. Procaccia, and S. Sela, J. Stat. Phys. **125**, 1029 (2006).
[5] Y. Tanaka, K. Fukao, Y. Miyamoto, and K. Sekimoto, Europhys. Lett. **43**, 664 (1998).
[6] Y. Tanaka, K. Fukao, and Y. Miyamoto, Eur. Phys. J. E **3**, 395 (2000).
[7] A.N. Gent and C.T.R. Pulford, J. Mat. Sci. **19**, 3612 (1984).
[8] A. Livine, G. Cohen, and J. Fineberg, Phys. Rev. Lett. **94**, 224301 (2005).
[9] C.-Y. Hui, A. Jagota, S.J. Bennison, and J. D. Londono, Proc. Roy. Soc. Lond. A **459**, 1489 (2003).
[10] T. Baumberger, C. Caroli, D. Martina, Nature Materials **5**, 552 (2006).
[11] T. Baumberger, C. Caroli, D. Martina, Eur. Phys. J. E **21**, 81 (2006).
[12] Computation of the real surface area shows it to differ by less than 1% from the apparent (projected) one, so that the corresponding correction to the fracture energy is negligible.
[13] A.N. Gent, Rubber Chem. Tech. **69**, 59 (1996).